International Journal of Automation and Computing 17(1), February 2020, 96-107
DOI: 10.1007/s11633-019-1176-9

Expression Analysis Based on Face Regions in Real-world Conditions

Zheng Lian[1,2] Ya Li[1] Jian-Hua Tao[1,2,3] Jian Huang[1,2] Ming-Yue Niu[1,2]

[1]National Laboratory of Pattern Recognition, Institute of Automation, Chinese Academy of Sciences (CAS), Beijing 100190, China

[2]School of Artificial Intelligence, University of Chinese Academy of Sciences, Beijing 100190, China

[3]CAS Center for Excellence in Brain Science and Intelligence Technology, Institute of Automation, Chinese Academy of Sciences, Beijing 100190, China

Abstract: Facial emotion recognition is an essential and important aspect of the field of human-machine interaction. Past research on facial emotion recognition focuses on the laboratory environment. However, it faces many challenges in real-world conditions, i.e., illumination changes, large pose variations and partial or full occlusions. Those challenges lead to different face areas with different degrees of sharpness and completeness. Inspired by this fact, we focus on the authenticity of predictions generated by different <emotion, region> pairs. For example, if only the mouth areas are available and the emotion classifier predicts happiness, then there is a question of how to judge the authenticity of predictions. This problem can be converted into the contribution of different face areas to different emotions. In this paper, we divide the whole face into six areas: nose areas, mouth areas, eyes areas, nose to mouth areas, nose to eyes areas and mouth to eyes areas. To obtain more convincing results, our experiments are conducted on three different databases: facial expression recognition + (FER+), real-world affective faces database (RAF-DB) and expression in-the-wild (ExpW) dataset. Through analysis of the classification accuracy, the confusion matrix and the class activation map (CAM), we can establish convincing results. To sum up, the contributions of this paper lie in two areas: 1) We visualize concerned areas of human faces in emotion recognition; 2) We analyze the contribution of different face areas to different emotions in real-world conditions through experimental analysis. Our findings can be combined with findings in psychology to promote the understanding of emotional expressions.

Keywords: Facial emotion analysis, face areas, class activation map, confusion matrix, concerned area.

1 Introduction

With the development of artificial intelligence, there is an explosion of interest in realizing more natural human-machine interaction (HMI) systems. Inspired by findings in psychology, Prendinger et al.[1], Martinovski and Traum[2] point out that addressing emotional information in the conversation of agents or the dialogue systems can enhance satisfaction and cause fewer breakdowns in the dialogue. Therefore, emotion recognition, as an essential aspect of HMI, is attracting more and more attention[3–5].

In the field of emotion recognition, facial expression recognition is a hot research topic due to its real-world applications. For example, there are millions of images that are being uploaded every day by different users. Their emotional states are useful for recommendation systems to determine whether to push product information. To automatically recognize the affective state of face images from the Internet, facial expression recognition is essential.

Past research on facial expression recognition is a multi-step process, where handicraft features are extracted first, combined with various classifiers and fusion methods. In general, facial features consist of two parts: appearance features and geometry features. As for appearance features, histogram of oriented gradient (HOG)[6], local binary patterns (LBP)[7], local phase quantization (LPQ)[8] and scale invariant feature transform (SIFT)[9] are widely utilized. As for geometry features, the head pose and landmarks are also considered in emotion recognition.

However, targets of the multi-step approach are not consistent. Besides, there is no agreement on appropriate handicraft features for emotion recognition. To solve these problems properly, the multi-step approach is replaced by the end-to-end method, which has gained state-of-the-art performance in many tasks, such as image classification[10], machine translation[11], scene classification[12], image caption generation[13] and speech synthesis[14]. In the end-to-end facial emotion recognition system, original faces cropped into standard size are treated as inputs. And, emotional labels are treated as outputs. End-to-end image classifiers, including AlexNet[15], visual geometry group (VGG)[16], GoogLeNet[17], ResNet[18], DenseNet[19]

Research Article
Manuscript received September 20, 2018; accepted March 8, 2019; published online April 23, 2019
Recommended by Associate Editor Bin Luo

and other variations of those models, are trained to map inputs to corresponding outputs.

Despite the great efforts that have been made to improve the performance of facial expression recognition, many challenges still exist. In real-world conditions, it′s difficult to gather faces without shade from other objects. Furthermore, faces are not always in the frontal pose and proper light conditions. Therefore, front faces without any noise are not always available in the emotion recognition task.

This question can be partially solved by conducting emotion recognition based on partial faces. The pioneer work by Ekman and Friesen.[20] proposed a facial action coding system (FACS), which described facial expression as the combination of multiple action units. Followed with [20], Tian et al.[21] focused on analyzing different facial parts, i.e., eyes, nose and mouth, and mapping them into action units (AU) coding. As for facial expression recognition, Wang et al.[22] combined FACS and LBP to represent facial expression features from coarse to fine. The facial feature regions were extracted by FACS, and then LBP was used to represent expression features for enhancing the discriminant. Sun et al.[23] proposed to recognize facial expression based on regions of interest, which guided convolutional neural networks (CNNs) to focus on areas associated with the expression. Wei et al.[24] found the joint representation by considering the texture and landmark modality of facial images. They divided faces into different patches, and then concatenated these corresponding patches as individual vectors. Zaman et al.[25] proposed a feature selection process to represent facial feature contribution according to their variations. However, previous works did not analyze the contribution of different face areas for different emotions. Besides, they mainly focused on the lab-controlled environment.

Considering the limitation of previous works[20–25], in this paper, we focus on the authenticity of predictions generated by different ⟨emotion, region⟩ pairs in real-world settings. For example, if only the mouth areas are available and the emotion classifier predicts happiness, then how should we calculate the confidence scores of predictions? This question can be converted into another question: how much information about happiness can be expressed through mouth areas? This question mainly focuses on psychology, and few studies focus on it.

To solve this problem to some extent, we divide the whole face into six areas: nose areas, mouth areas, eyes areas, nose to mouth areas, nose to eyes areas and mouth to eyes areas. What′s more, we analyze the contribution of different face areas to different emotions in the real-world settings. And, we visualize concerned areas of human faces in emotion recognition through class activation mapping (CAM)[26]. To obtain more convincing results, our experiments are conducted on three different databases: FER+, RAF-DB and expression in-the-wild (ExpW) dataset. Our work has some similarities with Busso et al.[27]. They separate the whole face into the forehead, eyebrow, low eye, right check and left check, and then a separate classifier is implemented for each block. Their experiments are conducted in the lab-controlled environment. However, in our paper, experiments are conducted in real-world conditions. In the meantime, the whole face is divided into smaller parts and more evaluation approaches are adapted. It is reasonable to believe that our findings can promote the understanding of emotional expressions.

This paper is organized as follows. In Section 2, we describe the proposed system. Experimental setup and evaluation results are illustrated in Sections 3 and 4, respectively. In Section 5, we conclude the whole paper.

2 System description

In this section, the classification model and the visualization model are discussed in detail.

1) As for the classification model, we follow the VGG network.

2) As for the visualization model, we follow the DenseNet-BC architecture in [19]. Through the CAM technique in the visualization model, we can visualize activation parts of different inputs.

Although the visualization model can also be utilized for the classification, we figure out that our classification model can obtain higher classification accuracy than the visualization model. Therefore, we split our classification process and visualization process into two parts. The architecture of two models can be found in Figs. 1 and 2, respectively.

2.1 Classification model

As for the classification model, we follow the VGG architecture, which consists of multiple convolutional layers, max pooling layers and a fully-connected layer (FC). The inputs of the system are grey-scale images in 64×64 pixels and the outputs are normalized emotion probabilities.

The system architecture is shown in Fig. 1. This network increases the depth using an architecture with very small (3×3) convolution filters, whose convolutional stride is fixed to 1 pixel. Batch normalization[28] and ReLU[29] are also added after the convolutional layers. Batch normalization alleviates the gradient explosion problems and ReLU is chosen as the activation functions. The max-pooling layer is appended behind two or three convolutional layers, which is performed over a 2×2 pixel window with stride 2. After multiple convolutional layers and max-pooling layers, a FC layer is connected behind to generate emotion probabilities, whose output dimension is the same as the number of categories in the dataset.

2.2 Visualization model

In the visualization model, we follow the DenseNet-

Fig. 1 Flowchart of our classification system. Yellow boxes, green boxes and grey boxes denote the 2D convolutional layers, max pooling layers and fully-connected layers, respectively. The number inside of the yellow box is the number of filters. And the number of neurons of the grey box is the same as the number of categories. Color versions of the figures in this paper are available online.

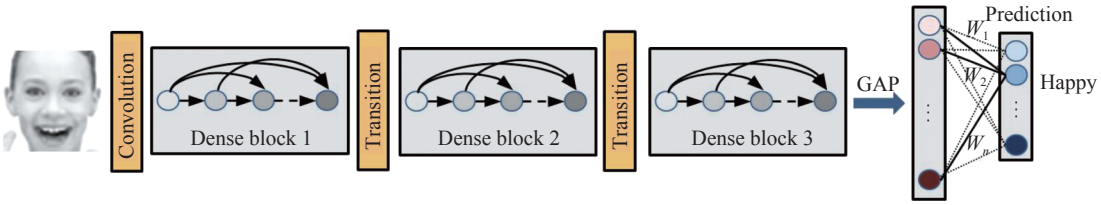

Fig. 2 Flowchart of our visualization system. Three dense blocks are followed behind the inputs, combining global average pooling (GAP) and a fully-connected layer in the end. The outputs of the system are normalized emotion probabilities.

BC architecture, which has three dense blocks associated with the global average pooling (GAP) and the FC behind. The inputs of the system are 64×64 grey-scale images and the outputs are normalized emotion probabilities.

The system architecture is shown in Fig. 2. Before entering into the first dense block, the convolutional layer with 16 output channels is performed on the 64×64 grey-scale images. Three dense blocks are followed behind and each dense block has 16 layers. In each dense block, 3×3 convolutional filters are used combining zero-padding with one pixel to keep the feature-map size fixed. Batch normalization is also added before convolutional layers to alleviate the gradient explosion problems. Between contiguous dense blocks, a transition block is applied to reduce the size and the channel of feature maps. The transition block is composed with a 1×1 convolutional layer, followed with 2×2 average pooling behind. Finally, the GAP and FC are combined to generate emotion probabilities.

2.3 The CAM technique

The CAM technique is adapted to visualize activation parts of different emotions, which projects back the weights of the output layer on to the convolutional feature maps to identify the importance of the image regions. Concretely, we utilize a weighted sum on the outputs of GAP, which are the spatial average of the feature maps generated from the last dense block.

We formulize the process of GAP as

$$F_k = \sum_{x,\ y} f_k(x,\ y) \tag{1}$$

where $f_k(x,\ y)$ represents the value of $(x,\ y)$ in the k-th feature map extracted from the last dense block. F^k represents the k-th output of GAP, which is spatial average of the k-th feature map.

To class c, the class score:

$$S_c = \sum_k w_k^c F_k = \sum_k w_k^c \sum_{x,\ y} f_k(x,\ y) = \sum_{x,\ y} \left(\sum_k w_k^c f_k(x,\ y) \right) \tag{2}$$

where w_k^c represents the value connected the k-th output of GAP to the class c.

Therefore, it is the CAM for inputs, which directly indicates importance of activation at spatial coordinate $(x,\ y)$ related to class c. By upsampling the CAM to the size of inputs, we can identify image regions, which are the most relevant to the particular category.

3 Experimental setup

Our system is tested on the FER+ dataset[30], RAF-DB dataset[31] and the ExpW dataset[32]. These datasets contain seven or eight emotion categories. Seven basic emotion categories, including neutral, happiness, surprise, sadness, anger, disgust and fear, are all contained in three datasets except that contempt is also considered in the FER+ dataset. These datasets are collected in read-world conditions and their emotions are more natural than existing databases[33–37]. In the meantime, their quantity is sufficient to train a robust deep network.

To divide the whole face into different facial parts, the open-source library, Dlib[38], is also utilized.

3.1 The FER+ database

The FER+ database is an extension of the FER database[39]. They re-label each image in the FER database through ten crowd taggers to overcome the noise label issue.

The FER dataset is created to mimic real-world conditions through the Google image search application programming interface (API). It consists of 35 887 images: 28 709 for the training, 3 589 for the public testing and 3 589 for the private testing. The dataset consists of

48×48 pixel grey-scale facial images. Each face is more or less centered and occupies about the same amount of space. The task is to categorize each face based on the emotion shown in the facial expression into one of seven categories, including neutral, happiness, surprise, sadness, anger, disgust and fear.

Compared with FER, FER+ has eight emotion categories adding contempt as well. We follow the same data selection method provided in [30]. If less than 50% of the votes are integrated, the sample will be removed. Then we combine the training data and the public testing set as the training set and evaluate the model performance on the private testing set. The data distribution of the training set and the testing set is shown in Table 1.

Table 1 Class category distribution of the FER+ dataset

	Train	Test	Total
Neutral	11000	1219	12219
Happiness	8326	920	9246
Surprise	3807	429	4236
Sadness	3660	421	4081
Anger	2535	287	2822
Disgust	151	19	170
Fear	636	88	724
Contempt	153	21	174
Sum	30268	3404	33672

3.2 The RAF-DB database

The RAF-DB database is a real-world expression database, which contains 29672 real-word facial images collected by the Flickr′s image search API. They employed 315 annotators who have been instructed with a one-hour tutorial on emotion for an online facial expression annotation assignment. Finally, each image was labeled by about 40 independent labelers. Subjects in the RAF-DB database range from 0 to 70 years old. There are 52% female, 43% male and 5% about which the annotators were unsure.

The RAF-DB database is divided into the single-label subset and the two-tab subset. The single-label subset contains seven classes of basic emotion, including neutral, happiness, surprise, sadness, anger, disgust and fear, and the two-tab subset contains twelve classes of compound emotions. In the experiment, we follow the same data selection method provided in RAF-DB and only utilize the single-label subset, which contains 15339 images: 12271 for the training and 3068 for the testing. The data distribution of the training set and the testing set is shown in Table 2.

3.3 The ExpW database

The ExpW database is a real-world expression database, which contains 91793 real-word facial images manually labeled with expressions. Each image in the ExpW dataset is labeled into one of seven basic categories: neutral, happiness, surprise, sadness, anger, disgust and fear.

Table 2 Class category distribution of the RAF-DB dataset

	Train	Test	Total
Neutral	2524	680	3204
Happiness	4772	1185	5957
Surprise	1290	329	1619
Sadness	1982	478	2460
Anger	705	162	867
Disgust	717	160	877
Fear	281	74	355
Sum	12271	3068	15339

Images in the ExpW dataset are collected by the Google image search API. At first, they combine a list of emotion-related keywords with different nouns as queries for Google image search. Then they collect images returned from the search engine and run a face detector[40]. Non-face images are removed. Images in the ExpW dataset have larger quantity and more diverse face variations than many databases.

The face confidence score is provided for each image in ExpW, which is range from 0 to 100. To analyze on a cleaner subset, we only choose face image whose confidence score is greater than 60 in the experiment. Since there is no existing separation approach for the training set and testing set, we split the dataset into the training set and testing set by a ratio of 4:1 while keeping the original label distribution. In the end, we utilize 33374 images in the ExpW for the experiment: 26701 for training and 6673 for testing. The data distribution of the training set and the testing set is shown in Table 3.

Table 3 Class category distribution of the ExpW dataset

	Train	Test	Total
Neutral	8309	2077	10386
Happiness	10576	2644	13220
Surprise	2471	617	3088
Sadness	2494	623	3117
Anger	1272	318	1590
Disgust	1250	312	1562
Fear	329	82	411
Sum	26701	6673	33374

3.4 Face region extraction

To divide facial images into different parts, facial landmark detection is essential. We utilize the open-source library, Dlib library, to detect landmarks, which takes the now classic HOG feature set combined with a linear classifier, an image pyramid and the sliding win-

dow detection scheme[41]. 68 landmarks are detected by Dlib, which can be found in Fig. 3.

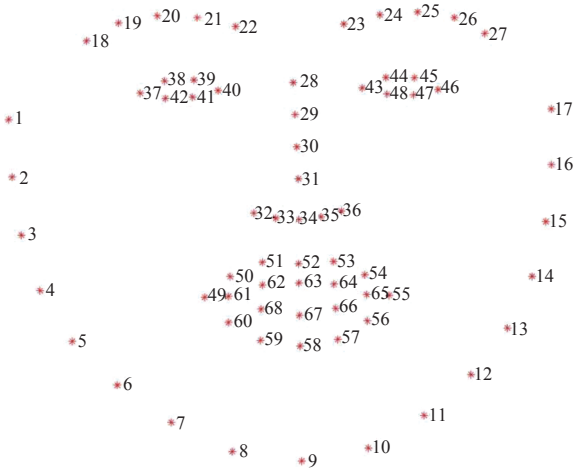

Fig. 3 68 landmarks that are detected by the Dlib library

After landmark extraction, we divide the whole face into six face regions based on the position of corresponding landmarks, including nose areas, mouth areas, eyes areas, nose to mouth areas, nose to eyes areas and mouth to eyes areas. In the division process, we utilize a "mask" to contain all landmarks of corresponding regions. Landmarks that should be contained for each region can be found in Table 4, whose index is the same as the index in Fig. 3. For example, the mouth region should contain 49th–68th landmarks.

Table 4 Landmarks for each region

Face areas	Landmark index
Mouth	[49, 68]
Nose	[29, 36]
Eyes	[18, 22] + [37, 42]
Nose and mouth	[29, 36] + [49, 68]
Nose and eyes	[18, 22] + [29, 36] + [37, 42]
Mouth and eyes	[18, 22] + [49, 68] + [37, 42]
The whole face	[1, 68]

Finally, an example of the division process is shown in Fig. 4. Through analysis of Fig. 4, we can figure out that $|width\text{-}height|$ values of different face regions are always greater than 0, especially for eyes areas, mouth areas and eyes to nose areas. This increases the challenges of the emotion recognition process. Therefore, data preprocessing approaches should to be chosen carefully, which is discussed in Section 4.1 in detail.

4 Evaluation results

In this section, we analyze the contribution of different face areas on three datasets: FER+, RAF-DB and ExpW.

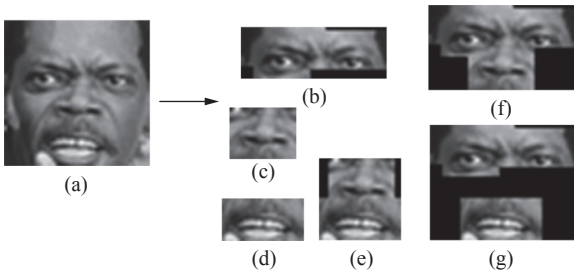

Fig. 4 The whole face (a) is divided into six face regions according to landmarks, including (b) eyes areas, (c) nose areas, (d) mouth areas, (e) nose to mouth areas, (f) nose to eyes areas and (g) mouth to eyes areas.

Firstly, we compare two data pre-processing methods, and choose the training approach and the testing approach for both classification model in Section 2.1 and visualization model in Section 2.2. Secondly, we analyze classification performance based on the whole face, which is calculated by the classification model in Section 2.1. We treat it as a comparison experiment. Thirdly, we visualize activation parts of the inputs through the CAM technique, which is based on the visualization model in Section 2.2. Finally, we compare the generation performance of models trained by seven face areas through the classification accuracy and the confusion matrix, and we also analyze the contribution of different face areas to different emotions.

4.1 Training and testing approach

To recognize emotions and visualize activation parts, we train the system for both the visualization model and the classification model.

In the training process, the Adam[42] optimizer is utilized to minimize the cross entropy loss. The learning rate is set to be 0.05 at first. If the classification accuracy of the testing dataset is decreased, a smaller learning rate will be utilized. As for the data augmentation methods, random crop original inputs into squares and random horizontal flip are chosen to obtain more robust emotion classifiers. Then, each image is normalized to have the same mean and variance in each channel. The maximum training epoch is set to be 100 and early stopping is applied to alleviate overfitting problems. To alleviate the randomness in the training process, we train the system five times and choose the best model according to the performance on the testing set.

In the testing process, data augmentation methods in the training process are replaced. Each face is cropped around the center.

As different images have different widths and heights, their aspect ratio is distinct, especially for cropped face regions such as mouth areas, whose $|width\text{-}height|$ is big.

If those images are cropped into squares in the data argumentation process, they will lose much information. Therefore, we utilize a padding approach to convert original inputs into standard images whose $|width\text{-}height|$ are 0.

To verify the effectiveness of the padding process, we compare classification accuracy on the RAF-DB dataset on two conditions: with padding and without padding. Classification accuracy can be found in Table 5.

Table 5 Classification accuracy (%) of the RAF-DB testing dataset at two conditions: with padding and without padding

Face areas	Non-padding	Padding
Mouth	55.12	60.07
Nose	44.43	49.02
Eyes	40.16	50.20
Nose and mouth	56.68	63.14
Nose and eyes	58.41	58.87
Mouth and eyes	67.63	67.83
The whole face	77.31	82.69

Through analysis of Table 5, we can figure out that the padding approach is useful for training a better system. Therefore, we will utilize the padding approach in the following experiments.

4.2 Performance of the whole face

To analyze the generation ability of trained models, we visualize the classification probabilities of the testing dataset through the confusion matrix, which is generated by the classification model in Section 2.1. Furthermore, we treat outputs of GAP in the visualization model in Section 2.2 as bottleneck features. And, we visualize these features through t-SNE[43], which is realized under scikit[44]. The confusion matrixes and t-SNE results are shown in Fig. 5. The same phenomenon can be found through two analysis methods.

We can figure out that the recognition performance of disgust and fear are bad through the confusion matrix in Fig. 5 (c). Besides, we can figure out that different emotion categories have a large overlap with others in t-SNE results. However, the confusion matrix and t-SNE results in Figs. 5 (a) and 5 (b) are better than Fig. 5 (c). Therefore, we are convinced that models trained by the FER+ dataset and the RAF-DB dataset have better generation performance than the ExpW dataset, which is related to the quality of labeling approach of each dataset.

Through further analysis of three confusion matrixes in Fig. 5, we can find that happiness always has the highest classification accuracy. Besides happiness, anger, sadness, surprise and neutral also have good performance. However, fear and disgust always have worse performance than other emotions. Such phenomena are related with unbalanced label distribution. In the meantime, it is also related with the definition of each emotion. The definition of happiness is clear and definite for most people. However, the definition of fear and disgust are blurred. Different people can mistake fear and disgust for different emotions. In the FER+ database, fear is easily confused with surprised and sadness, and disgust is easily confused with neutral and happiness. As for the RAF-DB dataset, the definition of fear and surprise are blurred. And, the disgust is easily mistaken for neutral and anger. In the ExpW dataset, disgust is easily confused with sadness and fear is easily confused with surprise.

Through analysis of three different datasets, we can find that fear and surprise are always easily confused with each other, which is related with the human perceptions of fear and surprise. The borderline of fear and surprise are quite blurred. Some emotions contain both fear and surprise, such as fright. Through Plutchik′s three-dimensional emotion model in [45], we can also find the same phenomenon that fear and surprise are close to each other in psychology.

As contempt only appears in the FER+ dataset and only few samples are labeled as contempt, the result of contempt is lack of confidence. Therefore, contempt is ignored in the following experiments.

4.3 CAM visualization

We visualize facial activation areas through CAM for CNNs with GAP. The heatmap is visualized through COLORMAP_JET color mapping realized under opencv, which varies from blue (low range) to green (mid range) to red (upper range). To show heatmaps on original images, we combine them together through weighted coefficient in [26]:

$$result = heatmap \times 0.4 + image \times 0.5. \tag{3}$$

Heatmaps of different emotions in three datasets are shown in Fig. 6.

As mouth areas, nose areas and eye areas are colored in most cases in Figs. 6 (a)–6 (c), we can infer that those areas are related with emotional expression. In the meantime, there are few colors on the forehead and cheek, which shows that the forehead and cheek have less contribution to emotional expressions.

As the red refers higher activation values than the blue, we can further figure out that mouth areas convey more emotional information than nose areas and eye areas, as heatmaps for mouth regions are close to red.

As for happiness, mouth areas are always colored in red, and eyes areas and nose areas are always colored in blue on three datasets. It shows that happiness is related with mouth areas in most cases. And eyes areas and nose areas contribute less than mouth areas for the happiness.

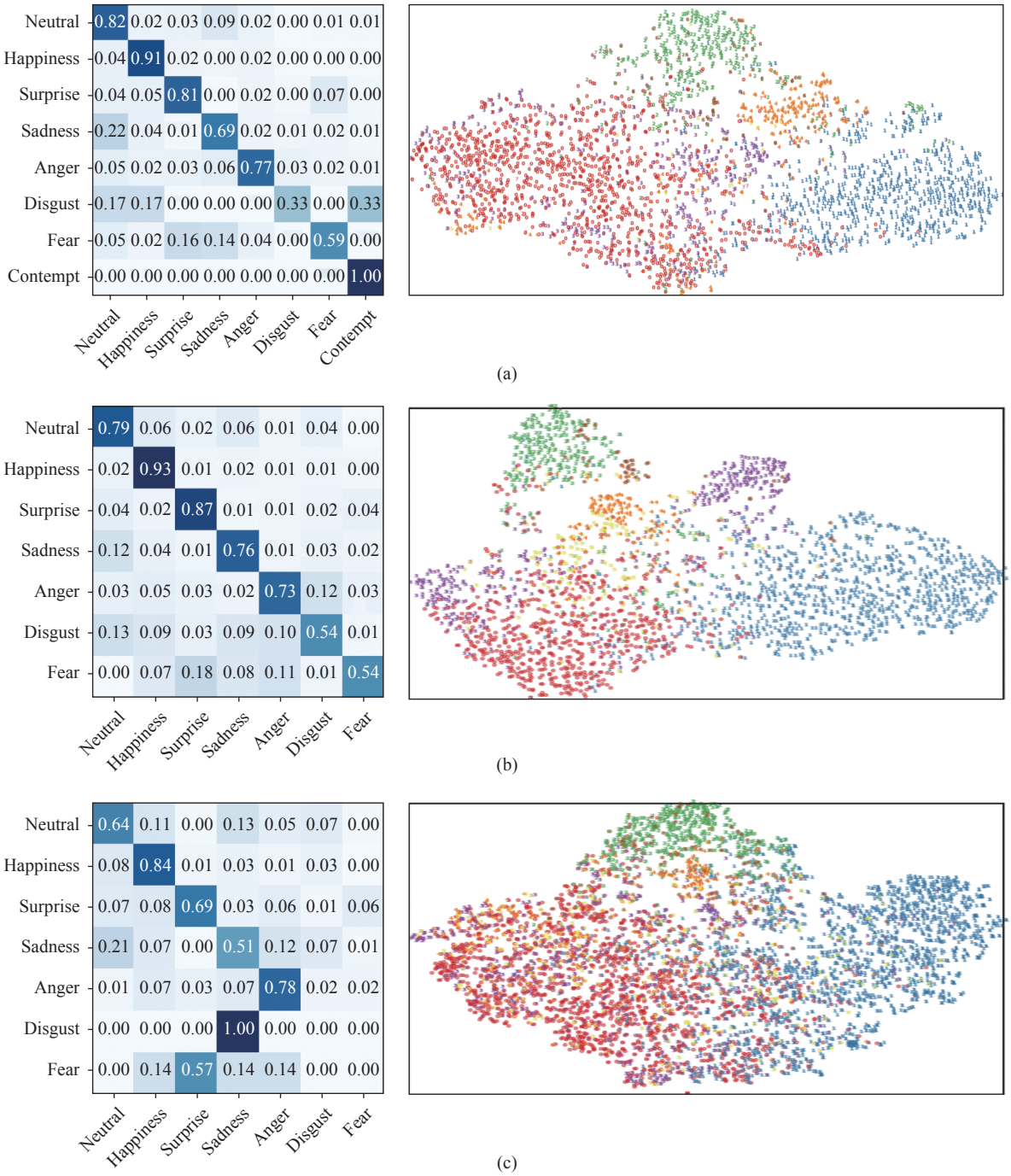

Fig. 5 Visualization the performance of models trained on three different databases. (a) The performance of the FER+ testing dataset based on the whole faces. Left: Visualising the confusion matrix; Right: Visualising of bottleneck features through t-SNE. (b) The performance of the RAF-DB testing dataset based on the whole faces. Left: Visualising the confusion matrix; Right: Visualising of bottleneck features through t-SNE. (c) The performance of the ExpW testing dataset based on the whole faces. Left: Visualising the confusion matrix; Right: Visualising of bottleneck features through t-SNE. [0(red): neutral, 1(blue): happiness, 2(green): surprise, 3(purple): sadness, 4(orange): anger, 5(yellow): disgust, 6(brown): fear, 7(pink): contempt]

As eyes areas and mouth areas are always colored in red for fear (and surprise), this shows that eyes areas and mouth areas convey more information than nose areas.

As for disgust and anger, those findings are related with the whole faces. Multiple face regions contribute to generate disgust and anger.

4.4 Contribution of different face areas

To compare the impact of different face areas, we train seven classification models based on seven face areas, including nose areas, mouth areas, eyes areas, nose to mouth areas, nose to eyes areas, mouth to eyes areas and the whole face areas. The training process and the

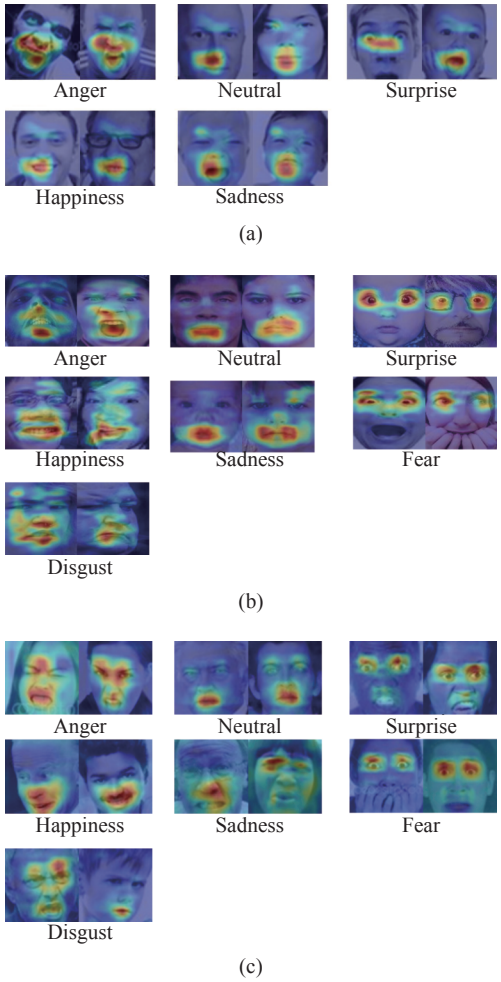

Fig. 6 Heatmaps of different emotions. (a) Results on the FER+ Database. (b) Results on the RAF-DB Database. (c) Results on the ExpW Database.

testing process followed with Section 4.1 except inputs are replaced by corresponding face regions. For example, as for mouth areas, we only utilize the mouth for both training and testing, and corresponding emotion labels are treated as outputs.

Our experiments are conducted on three datasets. Classification performance for seven face areas in the testing set is shown in Table 6. We also visualize the confusion matrix of the testing set for mouth, nose and eyes areas in Fig. 7.

Table 6 Classification accuracy (%) of different face areas in the testing set

Face areas	FER+	RAD-DB	ExpW
Mouth	73.17	60.07	64.53
Nose	68.81	49.02	53.51
Eyes	55.21	50.20	56.48
Nose and mouth	77.01	63.14	66.96
Nose and eyes	77.29	58.87	61.46
Mouth and eyes	81.57	67.83	67.27
The whole face	81.93	82.69	71.90

Through analysis of Table 6 and Fig. 7, we can figure out that compound regions (such as nose and mouth areas) always have better classification performance than corresponding basic areas (such as nose areas or mouth areas). In the meantime, the whole face areas always achieve the highest classification accuracy among seven face regions. Therefore, it is reasonable to conclude that the expression approach for each emotion is related to the whole face. And taking into account larger face areas is helpful to judge expressions more precisely.

As mouth areas have the highest classification accuracy among basic areas through analysis of Table 6, we can figure out that the mouth areas convey a lot of information about facial emotions.

As for the neutral, happiness and anger, mouth areas always gain the highest classification accuracy among basic areas through analysis of Fig. 7. It is reasonable to conclude that expression approaches for those emotions are related with mouth areas.

As for surprise, eyes areas lead to the least confusion among basic areas in most cases. We can figure out that the eyes areas contain much information about surprise.

5 Conclusions

Facial expression recognition is an essential part of the field of human-machine interaction. However, it faces many challenges in real-world conditions, such as illumination changes, large pose variations and partial or full occlusions. Those challenges lead to different face areas with different degrees of sharpness and completeness. Therefore, we focus on answering the emotion recognition confidence based on partial faces through analysis of the contribution of different face areas to different emotions, including nose areas, mouth areas, eyes areas, nose to mouth areas, nose to eyes areas, mouth to eyes areas and the whole face.

Through analysis of the confusion matrix, CAM results and the classification accuracy on three different datasets (including the FER+ dataset, the RAF-DB dataset and the ExpW dataset), we can figure out universal approaches for different emotional expressions. We learn that the mouth areas convey a lot of information about facial emotions, especially for the neutral, happiness and anger. The eye areas contain much information about surprise. Furthermore, we can judge expressions more precisely through considering larger face areas.

Our work can be combined with findings in the psychology. The contribution of this paper is critical to the study of human behaviors, and it can also promote the understanding of emotional expressions.

Acknowledgments

This work is supported by the National Key Research

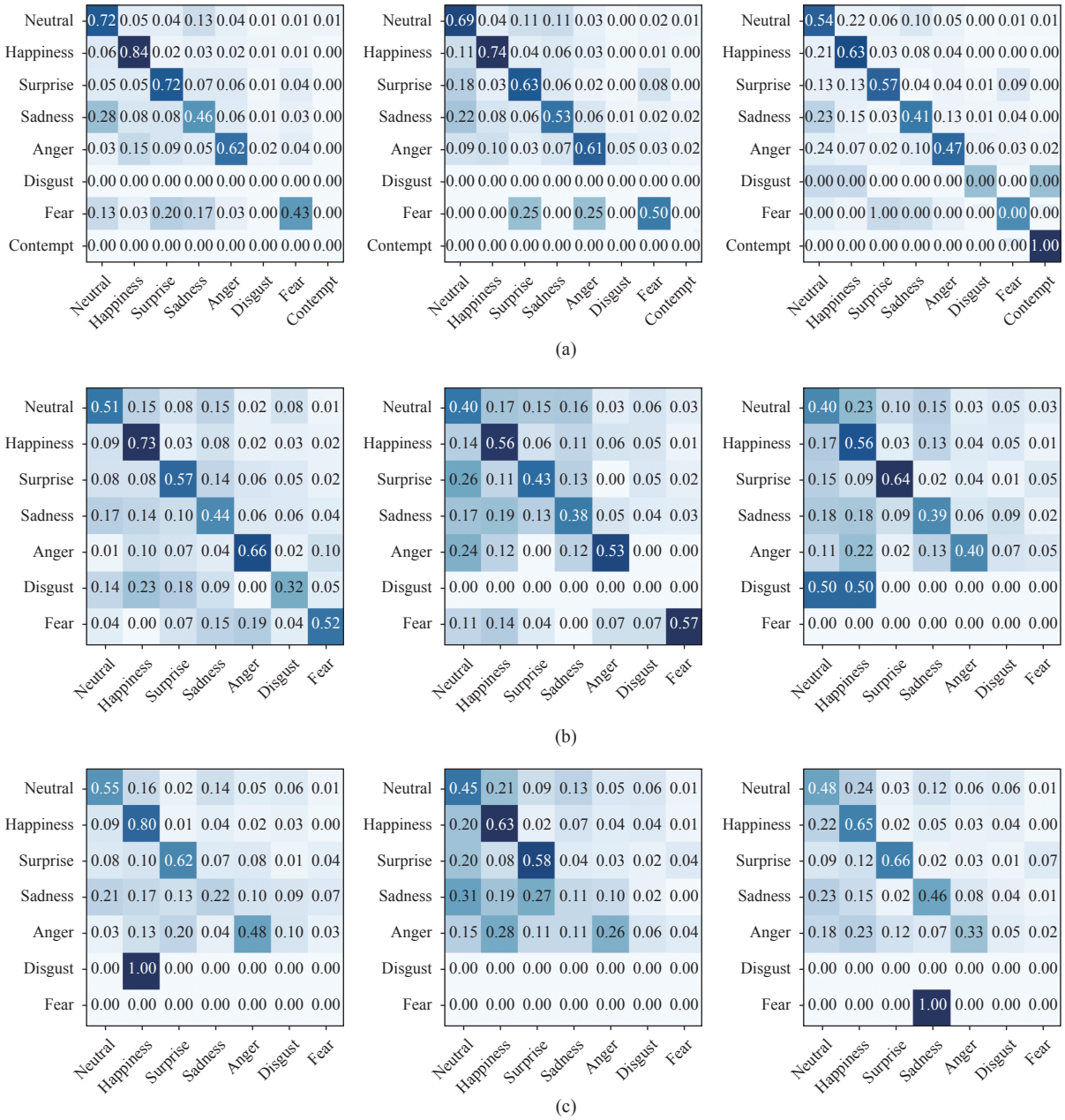

Fig. 7 Visualization the performance of different facial areas via confusion matrices. (a) The performance of the FER+ testing dataset: The confusion matrix based on mouth areas (the left column), nose areas (the middle column) and eyes areas (the right column). (b) The performance of the RAF-DB testing dataset: The confusion matrix based on mouth areas (the left column), nose areas (the middle column) and eyes areas (the right column). (c) The performance of the ExpW testing dataset: The confusion matrix based on mouth areas (the left column), nose areas (the middle column) and eyes areas (the right column).

& Development Plan of China (No. 2017YFB1002804), and National Natural Science Foundation of China (Nos. 61425017, 61773379, 61332017, 61603390 and 61771472) and the Major Program for the 325 National Social Science Fund of China (No. 13&ZD189).

References

[1] H. Prendinger, J. Mori, M. Ishizuka. Using human physiology to evaluate subtle expressivity of a virtual quizmaster in a mathematical game. *International Journal of Human-Computer Studies*, vol. 62, no. 2, pp. 231–245, 2005. DOI: 10.1016/j.ijhcs.2004.11.009.

[2] B. Martinovski, D. Traum. The error is the clue: Breakdown in human-machine interaction. In *Proceedings of the ISCA Tutorial and Research Workshop Error Handling in Spoken Dialogue Systems*, Château d'Oex, Switzerland, pp. 11–16, 2003.

[3] N. Asghar, P. Poupart, J. Hoey, X. Jiang, L. L. Mou. Affective neural response generation. In *Proceedings of the 40th European Conference on Information Retrieval Research*, Springer, Grenoble, France, pp. 154–166, 2017. DOI: 10.1007/978-3-319-76941-7_12.

[4] H. Zhou, M. L. Huang, T. Y. Zhang, X. Y. Zhu, B. Liu.

Emotional chatting machine: Emotional conversation generation with internal and external memory. In *Proceedings of the 32nd AAAI Conference on Artificial Intelligence*, New Orleans, USA, 2018.

[5] S. Ghosh, M. Chollet, E. Laksana, L. P. Morency, S. Scherer. Affect-LM: A neural language model for customizable affective text generation. In *Proceedings of the 55th Annual Meeting of the Association for Computational Linguistics*, ACL, Vancouver, Canada, pp. 634–642, 2017. DOI: 10.18653/v1/P17-1059.

[6] N. Dalal, B. Triggs. Histograms of oriented gradients for human detection. In *Proceedings of IEEE Computer Society Conference on Computer Vision and Pattern Recognition*, San Diego, USA, pp. 886–893, 2005. DOI: 10.1109/CVPR.2005.177.

[7] T. Ojala, M. Pietikainen, T. Maenpaa. Multiresolution gray-scale and rotation invariant texture classification with local binary patterns. *IEEE Transactions on Pattern Analysis and Machine Intelligence*, vol. 24, no. 7, pp. 971–987, 2002. DOI: 10.1109/TPAMI.2002.1017623.

[8] V. Ojansivu, J. Heikkilä. Blur insensitive texture classification using local phase quantization. In *Proceedings of the 3rd International Conference on Image and Signal Processing*, Springer, Cherbourg-Octeville, France, pp. 236–243, 2008. DOI: 10.1007/978-3-540-69905-7_27.

[9] D. G. Lowe. Distinctive image features from scale-invariant keypoints. *International Journal of Computer Vision*, vol. 60, no. 2, pp. 91–110, 2004. DOI: 10.1023/B:VISI.0000029664.99615.94.

[10] Y. P. Chen, J. N. Li, H. X. Xiao, X. J. Jin, S. C. Yan, J. S. Feng. Dual path networks. In *Proceedings of the 31st International Conference on Neural Information Processing Systems*, Curran Associates Inc., Long Beach, USA, pp. 4467–4475, 2017.

[11] A. Vaswani, N. Shazeer, N. Parmar, J. Uszkoreit, L. Jones, A. N. Gomez, L. Kaiser, I. Polosukhin. Attention is all you need. In *Proceedings of the 31st Conference on Neural Information Processing Systems*, Curran Associates, Inc., Long Beach, USA, pp. 6000–6010, 2017.

[12] L. Shen, Z. C. Lin, Q. M. Huang. Relay backpropagation for effective learning of deep convolutional neural networks. In *Proceedings of the 14th European Conference on Computer Vision*, Springer, Amsterdam, The Netherlands, pp. 467–482, 2016. DOI: 10.1007/978-3-319-46478-7_29.

[13] L. Chen, H. W. Zhang, J. Xiao, L. Q. Nie, J. Shao, W. Liu, T. S. Chua. SCA-CNN: Spatial and channel-wise attention in convolutional networks for image captioning. In *Proceedings of IEEE Conference on Computer Vision and Pattern Recognition*, Honolulu, USA, pp. 5659–5667, 2017. DOI: 10.1109/CVPR.2017.667.

[14] A. Van Den Oord, S. Dieleman, H. Zen, K. Simonyan, O. Vinyals, A. Graves, N. Kalchbrenner, A. Senior, K. Kavukcuoglu. Wavenet: A generative model for raw audio. In *Proceedings of the 9th ISCA Speech Synthesis Workshop*, Sunnyvale, USA, 2016.

[15] A. Krizhevsky, I. Sutskever, G. E. Hinton. ImageNet classification with deep convolutional neural networks. In *Proceedings of the 25th International Conference on Neural Information Processing Systems*, Curran Associates Inc., Lake Tahoe, Nevada, pp. 1097–1105, 2012.

[16] K. Simonyan, A. Zisserman. *Very Deep Convolutional Networks for Large-scale Image Recognition*, [Online], Available: https://arxiv.org/pdf/1409.1556.pdf, September, 2014.

[17] C. Szegedy, W. Liu, Y. Q. Jia, P. Sermanet, S. Reed, D. Anguelov, D. Erhan, D. Erhan, V. Vanhoucke, A. Rabinovich. Going deeper with convolutions. In *Proceedings of Conference on Computer Vision and Pattern Recognition*, Boston, USA, pp. 1–9, 2015. DOI: 10.1109/CVPR.2015.7298594.

[18] K. M. He, X. Y. Zhang, S. Q. Ren, J. Sun. Deep residual learning for image recognition. In *Proceedings of IEEE Conference on Computer Vision and Pattern Recognition*, Las Vegas, USA, pp. 770–778, 2016. DOI: 10.1109/CVPR.2016.90.

[19] G. Huang, Z. Liu, L. van der Maaten, K. Q. Weinberger. Densely connected convolutional networks. In *Proceedings of IEEE Conference on Computer Vision and Pattern Recognition*, Honolulu, USA, pp. 2261–2269, 2017. DOI: 10.1109/CVPR.2017.243.

[20] P. Ekman, W. V. Friesen. *The Facial Action Coding System (FACS): A Technique for the Measurement of Facial Action*, Palo Alto, USA: Consulting Psychologists, 1978.

[21] Y. I. Tian, T. Kanade, J. F. Cohn. Recognizing action units for facial expression analysis. *IEEE Transactions on Pattern Analysis and Machine Intelligence*, vol. 23, no. 2, pp. 97–115, 2001. DOI: 10.1109/34.908962.

[22] L. Wang, R. F. Li, K. Wang, J. Chen. Feature representation for facial expression recognition based on FACS and LBP. *International Journal of Automation and Computing*, vol. 11, no. 5, pp. 459–468, 2014. DOI: 10.1007/s11633-014-0835-0.

[23] X. Sun, M. Lv, C. Q. Quan, F. J. Ren. Improved facial expression recognition method based on ROI deep convolutional neutral network. In *Proceedings of the 7th International Conference on Affective Computing and Intelligent Interaction*, IEEE, San Antonio, USA, pp. 256–261, 2017. DOI: 10.1109/ACII.2017.8273609.

[24] Z. Wei, Y. M. Zhang, L. Ma, J. W. Guan, S. J. Gong. Multimodal learning for facial expression recognition. *Pattern Recognition*, vol. 48, no. 10, pp. 3191–3202, 2015. DOI: 10.1016/j.patcog.2015.04.012.

[25] F. K. Zaman, A. A. Shafie, Y. M. Mustafah. Robust face recognition against expressions and partial occlusions. *International Journal of Automation and Computing*, vol. 13, no. 4, pp. 319–337, 2016. DOI: 10.1007/s11633-016-0974-6.

[26] B. L. Zhou, A. Khosla, A. Lapedriza, A. Oliva, A. Torralba. Learning deep features for discriminative localization. In *Proceedings of IEEE Conference on Computer Vision and Pattern Recognition*, Las Vegas, USA, pp. 2921–2929, 2016. DOI: 10.1109/CVPR.2016.319.

[27] C. Busso, Z. G. Deng, S. Yildirim, M. Bulut, C. M. Lee, A. Kazemzadeh, S. Lee, U. Neumann, S. Narayanan. Analysis of emotion recognition using facial expressions, speech and multimodal information. In *Proceedings of the 6th International Conference on Multimodal Interfaces*, ACM, State College, USA, pp. 205–211, 2004. DOI: 10.1145/1027933.1027968.

[28] S. Ioffe, C. Szegedy. Batch normalization: Accelerating deep network training by reducing internal covariate shift. In *Proceedings of the 32nd International Conference on Machine Learning*, Curran Associates, Inc., Lille, France, pp. 448–456, 2015.

[29] K. Jarrett, K. Kavukcuoglu, M. A. Ranzato, Y. LeCun. What is the best multi-stage architecture for object recognition?. In *Proceedings of the 12th IEEE International Conference on Computer Vision*, Kyoto, Japan, pp. 2146–

2153, 2010. DOI: 10.1109/ICCV.2009.5459469.

[30] E. Barsoum, C. Zhang, C. C. Ferrer, Z. Y. Zhang. Training deep networks for facial expression recognition with crowd-sourced label distribution. In *Proceedings of the 18th ACM International Conference on Multimodal Interaction*, Tokyo, Japan, pp. 279–283, 2016. DOI: 10.1145/2993148.2993165.

[31] S. Li, W. H. Deng, J. P. Du. Reliable crowdsourcing and deep locality-preserving learning for expression recognition in the wild. In *Proceedings of IEEE Conference on Computer Vision and Pattern Recognition*, Honolulu, USA, pp. 2584–2593, 2017. DOI: 10.1109/CVPR.2017.277.

[32] Z. P. Zhang, P. Luo, C. C. Loy, X. O. Tang. From facial expression recognition to interpersonal relation prediction. *International Journal of Computer Vision*, vol. 126, no. 5, pp. 550–569, 2018. DOI: 10.1007/s11263-017-1055-1.

[33] M. J. Lyons, J. Budynek, S. Akamatsu. Automatic classification of single facial images. *IEEE Transactions on Pattern Analysis and Machine Intelligence*, vol. 21, no. 12, pp. 1357–1362, 1999. DOI: 10.1109/34.817413.

[34] M. Pantic, M. Valstar, R. Rademaker, L. Maat. Web-based database for facial expression analysis. In *Proceedings of IEEE International Conference on Multimedia and Expo*, Amsterdam, Netherlands, 2005. DOI: 10.1109/ICME.2005.1521424.

[35] G. Y. Zhao, X. H. Huang, M. Taini, S. Z. Li, M. Pietikäinen. Facial expression recognition from near-infrared videos. *Image and Vision Computing*, vol. 29, no. 9, pp. 607–619, 2011. DOI: 10.1016/j.imavis.2011.07.002.

[36] P. Lucey, J. F. Cohn, T. Kanade, J. Saragih, Z. Ambadar, I. Matthews. The Extended Cohn-Kanade Dataset (CK+): A complete dataset for action unit and emotion-specified expression. In *Proceedings of IEEE Computer Society Conference on Computer Vision and Pattern Recognition-Workshops*, San Francisco, USA, pp. 94–101, 2010. DOI: 10.1109/CVPRW.2010.5543262.

[37] A. Dhall, O. V. Ramana Murthy, R. Goecke, J. Joshi, T. Gedeon. Video and image based emotion recognition challenges in the wild: EmotiW 2015. In *Proceedings of the ACM on International Conference on Multimodal Interaction*, Seattle, USA, pp. 423–426, 2015. DOI: 10.1145/2818346.2829994.

[38] D. E. King. Dlib-ml: A machine learning toolkit. *Journal of Machine Learning Research*, vol. 10, pp. 1755–1758, 2009.

[39] I. J. Goodfellow, D. Erhan, P. L. Carrier, A. Courville, M. Mirza, B. Hamner, W. Cukierski, Y. C. Tang, D. Thaler, D. H. Lee, Y. B. Zhou, C. Ramaiah, F. X. Feng, R. F. Li, X. J. Wang, D. Athanasakis, J. Shawe-Taylor, M. Milakov, J. Park, R. Ionescu, M. Popescu, C. Grozea, J. Bergstra, J. J. Xie, L. Romaszko, B. Xu, Z. Chuang, Y. Bengio. Challenges in representation learning: A report on three machine learning contests. *Neural Networks*, vol. 64, pp. 59–63, 2015. DOI: 10.1016/j.neunet.2014.09.005.

[40] B. Yang, J. J. Yan, Z. Lei, S. Z. Li. Aggregate channel features for multi-view face detection. In *Proceedings of IEEE International Joint Conference on Biometrics*, Clearwater, USA, pp. 1–8, 2014. DOI: 10.1109/BTAS.2014.6996284.

[41] V. Kazemi, J. Sullivan. One millisecond face alignment with an ensemble of regression trees. In *Proceedings of IEEE Conference on Computer Vision and Pattern Recognition*, Columbus, USA, pp. 1867–1874, 2014. DOI: 10.1109/CVPR.2014.241.

[42] D. P. Kingma, J. Ba. *Adam: A Method for Stochastic Optimization*, [Online], Available: https://arxiv.org/pdf/1409.1556.pdf, September, 2014.

[43] L. van der Maaten, G. Hinton. Visualizing data using t-SNE. *Journal of Machine Learning Research*, vol. 9, pp. 2579–2605, 2008.

[44] F. Pedregosa, G. Varoquaux, A. Gramfort, V. Michel, B. Thirion, O. Grisel, M. Blondel, P. Prettenhofer, R. Weiss, V. Dubourg, J. Vanderplas, A. Passos, D. Cournapeau, M. Brucher, M. Perrot, É. Duchesnay. Scikit-learn: Machine learning in python. *Journal of Machine Learning Research*, vol. 12, pp. 2825–2830, 2013.

[45] R. Plutchik. The multifactor-analytic theory of emotion. *Journal of Psychology*, vol. 50, no. 1, pp. 153–171, 1960. DOI: 10.1080/00223980.1960.9916432.

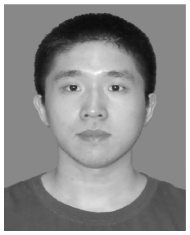

Zheng Lian received the B. Eng. degree in telecommunication from Beijing University of Posts and Telecommunications, China in 2016. He is a Ph. D. degree candidate in pattern recognition and intelligent system at the National Laboratory of Pattern Recognition (NLPR), Institute of Automation, Chinese Academy of Sciences, China.

His research interests include affective computing, deep learning and multimodal emotion recognition.

E-mail: lianzheng2016@ia.ac.cn

ORCID iD: 0000-0001-9477-0599

Ya Li received the B. Eng. degree in automation from University of Science and Technology of China (USTC), China in 2007, and the Ph. D. degree in pattern recognition and intelligent system from NLPR, Institute of Automation, Chinese Academy of Sciences (CASIA), China in 2012. She is currently an associate professor in CASIA, China. She has published more than 50 papers in the related journals and conferences, such as *Speech Communication, International Conference on Acoustics, Speech and Signal Processing (ICASSP), INTERSPEECH,* and *International Conference on Affective Computing and Intelligent Interaction (ACII)*. She has won the Second Prize of Beijing Science and Technology Award in 2014. She has also won the Best Student Paper in *Interspeech 2016*.

Her interests include affective computing and human-computer interaction.

E-mail: yli@nlpr.ia.ac.cn (Corresponding author)

ORCID iD: 0000-0002-6284-5039

Jian-Hua Tao received the Ph. D. degree in computer science from Tsinghua University, China in 2001. He is winner of the National Science Fund for Distinguished Young Scholars and the deputy director in NLPR, CASIA, China. He has directed many national projects, including "863", National Natural Science Foundation of China. He has published more than eighty papers on journals and proceedings including *IEEE Transactions on ASLP*, and *ICASSP, INTERSPEECH*. He also serves as the steering committee member for *IEEE Transactions on Affective Computing* and the chair or program committee member for major conferences, including *International Conference on*

Pattern Recognition (ICPR), Interspeech, etc.

His research interests include speech synthesis, affective computing and pattern recognition.

E-mail: jhtao@nlpr.ia.ac.cn

Jian Huang received the B. Eng. degree in automation from Wuhan University. China in 2015. He is a Ph. D. degree candidate in pattern recognition and intelligent system at the National Laboratory of Pattern Recognition (NLPR), Institute of Automation, Chinese Academy of Sciences, China. He had published the papers in *Interspeech* and *ICASSP*.

His research interests include affective computing, deep learning and multimodal emotion recognition.

E-mail: jian.huang@nlpr.ia.ac.cn

Ming-Yue Niu received the M. Sc. degree in information and computing science from Department of Applied Mathematics, Northwestern Polytechnical University (NWPU), China in 2017. Currently, he is a Ph. D. degree candidate in pattern recognition and intelligent system at the National Laboratory of Pattern Recognition (NLPR), Institute of Automation, Chinese Academy of Sciences (CASIA), China.

His research interests include affective computing and human-computer interaction.

E-mail: niumingyue2017@ia.ac.cn